Chaos-induced dynamical hysteresis: Energetic and entropic barriers

Moupriya Das and Deb Shankar Ray*
Indian Association for the Cultivation of Science, Jadavpur, Kolkata 700032, India
(Received 9 January 2013; published 15 March 2013)

We consider periodically driven dynamical systems with energetic and entropic barriers in the presence of deterministic noise. Due to the relaxational delay, the response of the system lags behind the applied field and exhibits dynamical hysteresis manifested in the nonvanishing area of the response-function–field loop. It is demonstrated that the hysteresis loop area satisfies a scaling law with exponents that depend on the nature of the barrier.

DOI: 10.1103/PhysRevE.87.032135 PACS number(s): 05.40.−a, 05.10.Gg, 05.45.−a

I. INTRODUCTION

Dynamical hysteresis is an interesting nonequilibrium phenomenon in driven cooperatively interacting many-body systems. It appears due to the delay in response of the system towards an external periodic signal in the presence of thermal fluctuation. The relaxational delay gives rise to a symmetry breaking in the response-function–field plot, although the external oscillating field does not provide any symmetry-breaking input [1]. As a result, a nonvanishing area of the response-function–field loop is obtained. Furthermore, the loop area vanishes in the very-low- and very-high-frequency limits exhibiting a maximum at an intermediate value of the frequency of oscillation. Dynamic hysteresis has been studied extensively in magnetic systems [2], stochastic systems [3], self-organizing avalanches [4], design engineering, and many other aspects [1–5]. We refer to [1] for further details.

To present the discussion in an appropriate context, we begin by noting that stochasticity plays a crucial role in dynamical hysteresis. This is because thermal noise directly influences the delay in the response of the many-body system. It would seem that the relaxational delay may play a similar role when the driven system is in contact with a dynamical system exhibiting deterministic stochasticity or chaos. In other words, we address the following question: Can a periodically driven system admit of dynamical hysteresis when it is coupled to a chaotic bath? The role of a chaotic system acting as a thermal bath or, more generally, an environment has been investigated earlier in several situations, including realizations of deterministic Brownian motion generated by a chaotic process [6]; several thermodynamically inspired quantities such as temperature [7], entropy production, and flux [8]; and statistical mechanics analogs [9] of the Kubo relation, the fluctuation-decoherence relation, and the fluctuation-dissipation relation [10] in chaotic systems. The focus of the present work is an investigation of dynamical hysteresis in a driven nonequilibrium system in the presence of a deterministic noise. We envisage two distinct situations. The first is when the system in question is governed by a double-well potential. The transitions caused by chaos between the two wells are guided by energetic considerations. In the second case we consider a system where the potential barrier is not energetic but entropic in origin. The entropic potential arises when the diffusive Brownian motion of particles through a tube of varying cross section in higher dimension is effectively reduced to one dimension [11].

Entropic potential [11–25] has been studied extensively and many novel phenomena such as entropic stochastic resonance [19], entropic resonant activation [20], entropic noise-induced nonequilibrium transition [18], and asymmetric stochastic localization in the case of geometry controlled kinetics [25] have been explored. The idea of entropic transport has also been employed in the case of entropic ratchet motion [21,26,27], mobility of particles [28,29], logical response in entropic transport [30], and in other contexts involving passage of particles through phospholipid membranes, biological channels [31], artificial ion pumps, and studies related to polymers [32–34], DNA translocation through nanostructures [35], and many other aspects [21–53]. These developments have potential implications in geometry-influenced physiochemical rate processes [54–56]. A similar kind of effect has been found in a model system that reveals that the stochastic resonance phenomenon can occur as an outcome of confinement [57,58]. The entropic potential appears as a result of the boundary effect of the system. In the present study we inquire whether this boundary effect is effective for the occurrence of dynamic hysteresis in a two-dimensional enclosure of varying cross section in the presence of deterministic noise rather than thermal noise. We show that when a particle confined in a two-dimensional bilobal enclosure is driven by an external time-periodic perturbation and kept in contact with a chaotic bath, the response function traces a hysteresis loop when plotted against the field. The turnover of the hysteresis loop area with the frequency of oscillation is also observed as a characteristic feature of dynamic hysteresis. It is thus evident that dynamic hysteresis can occur in the presence of fluctuations arising out of a chaotic bath. An interesting offshoot of this investigation is that the observed variation of the loop area with frequency in both cases follows a generic form as revealed through the scaling behavior. The present phenomena can be considered as deterministic analogs of energetic and entropic dynamic hystereses.

The paper is organized as follows. In Sec. II we discuss the essential dynamics of the chaotic bath that drives the system. The model and dynamics of the system are discussed for energetic and entropic barriers. To describe the energetic system, we consider a particle moving in a bistable potential field and subjected to an oscillating field and a chaotic bath.

*pcdsr@iacs.res.in

For an entropic system, we consider the motion of the particle in a two-dimensional bilobal confinement with varying cross section. In Sec. III we present a detailed description of numerical simulations and discuss the results. The paper is summarized in Sec. IV.

II. MODEL DESCRIPTION AND DYNAMICS OF THE SYSTEM

We consider a low-dimensional nonlinear system to model a chaotic bath. This comprises two interacting quartic oscillators characterized by a set of coordinates and momenta x, y and p_x, p_y, respectively. The Hamiltonian of the bath is given by

$$H_B = \frac{p_x^2 + p_y^2}{2} + \frac{a}{4}(x^4 + y^4) + \frac{x^2 y^2}{2}. \tag{2.1}$$

The equations of motion of the bath are

$$\dot{x} = p_x, \tag{2.2}$$

$$\dot{p_x} = -ax^3 - xy^2, \tag{2.3}$$

$$\dot{y} = p_y, \tag{2.4}$$

$$\dot{p_y} = -ay^3 - x^2 y, \tag{2.5}$$

where a is a dimensionless parameter. The variables x, y, p_x, p_y, and time t are made dimensionless with proper scaling factors. The parameter a governs the dynamics of the bath. Depending upon the value of a, the bath exhibits chaotic or regular behavior. For $a \to 0$ limit the dynamics of the bath is chaotic. The system is integrable for the special values of $a = 0.33$ and 1.0. We have used $a = 0.01$ throughout our study. The largest Lyapunov exponent is positive in this regime. Several variants of the model have been considered in earlier works for the exploration of energy transfer dynamics [59] and understanding the nature of thermalization [7,59]. Our aim here is to exploit the model as a source of deterministic noise to study dynamical hysteresis. Depending on the nature of coupling to the other degrees of freedom of the overall system, two distinct situations emerge.

A. System with energy barrier

We first consider the overdamped dynamics of a particle moving in a one-dimensional bistable potential field and subjected to an external periodic drive. The potential has the form

$$V(q) = \frac{a_1}{4}q^4 - \frac{b_1}{2}q^2. \tag{2.6}$$

The potential has one maximum at $q_{\max} = 0$ and two minima at $q_{\min} = \pm\sqrt{b_1/a_1}$, as shown in Fig. 1. The energy difference between the maximum and the minima $\Delta V = b_1^2/4a_1$ creates the energy barrier for the particle. The deterministic fluctuation is now injected in the system through the variable governed by the set of dynamical equations (2.2)–(2.5). The overdamped dynamics of the system can be expressed as

$$\Gamma\frac{dq}{dt} = -V'(q) + A_0\sin(\omega t) + cx, \tag{2.7}$$

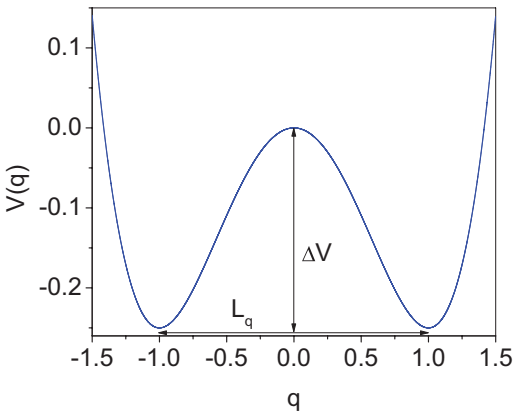

FIG. 1. (Color online) Double-well potential with system parameters $a_1 = 1.0$ and $b_1 = 1.0$.

where Γ is the frictional coefficient, q represents the position of the particle, $-V'(q)$ corresponds to the force field acting on the particle, A_0 and ω are the amplitude and frequency of the periodic driving, respectively, and c is a constant that denotes the strength of the coupling of the chaotic drive. To make Eq. (2.7) dimensionless we divide q by L_q, a characteristic length representing the distance between two minima of the bistable potential and time t by a characteristic time τ, representing the mean first-passage time of the particle from one potential minimum to the other. Thus the forces are scaled by the quantity $\frac{\Gamma L_q}{\tau}$. We can further define the dimensionless quantities as follows: $\tilde{q} = \frac{q}{L_q}$ is the dimensionless position variable of the particle, $\tilde{t} = \frac{t}{\tau}$ is the dimensionless time, $\tilde{a}_1$ and $\tilde{b}_1$ are the dimensionless coefficients (made dimensionless using proper scaling factors), $\tilde{A}_0$ has the form $\tilde{A}_0 = \frac{A_0\tau}{\Gamma L_q}$, the dimensionless frequency $\tilde{\omega}$ can be represented as $\tilde{\omega} = \omega\tau$, and the dimensionless parameter $\tilde{c}$ and variable $\tilde{x}$ have the forms $\tilde{c} = \frac{c\tau}{\Gamma}$ and $\tilde{x} = \frac{x}{L_q}$. For the sake of brevity and notational convenience, we omit the tilde from now on to represent dimensionless quantities. Now the dynamics of the system can be presented in the form

$$\frac{dq}{dt} = -a_1 q^3 + b_1 q + A_0\sin(\omega t) + cx. \tag{2.8}$$

In the following section we make use of Eqs. (2.2)–(2.5) and (2.8) for numerical simulations for the study of dynamical hysteresis for the energetic barrier. The quantity c has been taken to be equal to 1 for all the numerical calculations.

B. System with entropic barrier

Another part of our study concerns the motion of a particle in the presence of an entropic barrier. This barrier arises whenever there is a variation in the diameter of a tube or a channel for which the particle requires more time to travel from one point to the other. For a channel of uniform width, the problem of transport is essentially one dimensional. However, if there is a bulge, the motion of the particle slows down in the vicinity of it. This is because the particle can explore more space by its random walk. Again when there is a constriction in the channel, more time is required because the particle has to find its path through the bottleneck. Thus any variation in shape

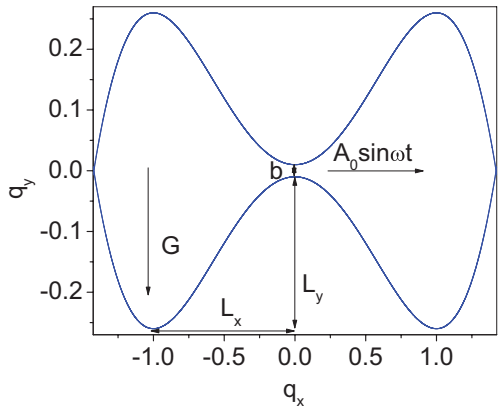

FIG. 2. (Color online) Two-dimensional bilobal system with system parameters $\epsilon = 0.25$ and $b = 0.02$.

retards the motion of the particle. When the system is driven by a white noise it is possible to formulate the stochastic dynamics of the particle in terms of the Fokker-Planck equation [60] in two dimensions. Zwanzig showed that for a tube of varying cross section, it is possible to reduce the stochastic dynamics to one-dimensional transport governed by the Fick-Jacobs equation and confinement in higher dimension gives rise to an entropic potential in lower dimension.

We now consider the problem of entropic transport when the noise has a deterministic origin according to Eqs. (2.2)–(2.5). The confinement is assumed to be a two-dimensional bilobal enclosure with varying cross section, as shown in Fig. 2. A particle is subjected to an external oscillatory drive in the x direction and a weak transverse force along the negative-y direction. The motion of the particle is governed by a drive from the chaotic bath discussed earlier. The overdamped two-dimensional motion of the particle can be expressed as

$$\Gamma\frac{d\vec{r}}{dt} = -G\hat{e}_y + A_0\sin(\omega t)\hat{e}_x + cx\hat{e}_x + cy\hat{e}_y, \qquad (2.9)$$

where $\vec{r}$ is the position vector of the particle, which can be expressed as $\vec{r} = q_x\hat{e}_x + q_y\hat{e}_y$, with q_x and q_y the position variables of the particle in the confinement along the x and y directions, respectively, and G is the weak force acting along the negative-y direction of the structure. A periodic force with amplitude A_0 acts on the particle along the longitudinal direction. Here x and y are the bath variables that introduce chaos into the system. For simplicity, we assume the same coupling strength c in both directions. The two-dimensional confinement can be imposed by using reflecting boundary conditions. The system boundary, as shown in Fig. 2, can be described by using

$$B_l(q_x) = -B_u(q_x) = L_y(q_x/L_x)^4 - 2L_y(q_x/L_x)^2 - b/2, \qquad (2.10)$$

where $B_l(x)$ and $B_u(x)$ are the expressions for the lower and upper boundaries of the system, respectively, L_x corresponds to the distance between the position of the middle point of the bottleneck and the maximal width of the structure, the length L_y represents the narrowing of the boundary function, and b is the remaining width at the bottleneck. Consequently, the local half-width of the system can be expressed as

$$B(q_x) = [B_u(q_x) - B_l(q_x)]/2. \qquad (2.11)$$

For convenience, we now make the dynamics dimensionless [15–25]. The length is made dimensionless using the characteristic length scale L_x and time by the characteristic time scale τ introduced earlier. The description of the dynamics is obtained by using the dimensionless quantities $\tilde{q}_x = q_x/L_x$ and $\tilde{q}_y = q_y/L_x$, implying $\tilde{b} = b/L_x$ and $\tilde{t} = t/\tau$. This ensures that the wall functions of the system are dimensionless, i.e., $\tilde{B}_l(\tilde{q}_x) = B_l(q_x)/L_x = -\tilde{B}_u(\tilde{q}_x)$ and $\tilde{B}(\tilde{q}_x) = B(q_x)/L_x$. The forces are scaled by the quantity $F_R = \Gamma L_x/\tau$. Thus we can write $\tilde{G} = G\tau/\Gamma L_x$ and $\tilde{A}_0 = A_0\tau/\Gamma L_x$. The scaled frequency $\tilde{\omega}$ takes the form $\tilde{\omega} = \omega\tau$. Here $\tilde{x}$ and $\tilde{y}$ can be represented as $\tilde{x} = x/L_x$ and $\tilde{y} = y/L_x$ and the dimensionless strength of the chaotic drive has the form $\tilde{c} = c\tau/\Gamma$. Again, for the sake of brevity we dispense with the tilde to represent scaled quantities. In dimensionless form, the dynamical equation of motion of the particle can be written as

$$\frac{d\vec{r}}{dt} = -G\hat{e}_y + A_0\sin(\omega t)\hat{e}_x + cx\hat{e}_x + cy\hat{e}_y. \qquad (2.12)$$

The dynamics of the system can be decomposed into two equations along the two perpendicular directions

$$\begin{aligned}\frac{dq_x}{dt} &= A_0\sin(\omega t) + cx,\\ \frac{dq_y}{dt} &= -G + cy.\end{aligned} \qquad (2.13)$$

Like the previous case, here also c has been taken to be equal to 1 for all the numerical calculations. The dimensionless boundary function has the form

$$B(q_x) = [B_u(q_x) - B_l(q_x)]/2 = -\epsilon q_x^4 + 2\epsilon q_x^2 + b/2, \qquad (2.14)$$

where $\epsilon = L_y/L_x$ is the aspect ratio. Thus ϵ is an appropriately scaled quantity. Now Eq. (2.13) and the equations of motion (2.2)–(2.5) for the chaotic bath form a system-reservoir couple. The confinement is introduced through the reflection of the particle at the boundary of the system [Eq. (2.14)].

III. NUMERICAL SIMULATIONS: RESULTS AND DISCUSSION

A. Hysteresis loops

Our aim here is to inquire whether a system with deterministic stochasticity admits dynamical hysteresis when driven by a periodic force. To this end, we define a response-function integrated probability of residence of particles in any one of the potential wells or in either of the lobes for the system with an energy or entropic barrier, respectively. We first consider the energetic case. Let the probability of finding a particle at position q and at time t be $P(q,t)$. Then the integrated probability of residence of the particles in one of the wells $P_i(t)$ is defined as

$$P_i(t) = \int_{q_{\max}}^{\pm q_r} dq\ P(q,t), \qquad (3.1)$$

where $i = L,R$ for the left and right wells, respectively, $q_{\max} = 0$ is the position of the maximum of the potential well,

and $\pm q_r$ correspond to the reflecting ends of the potential. The limit of integration runs from $q_{\max}$ to $-q_r$ to get the integrated probability of residence of particles in the left well and from $q_{\max}$ to q_r to get that for the right well. This integrated probability takes into account the total number of particles residing in either of the potential wells. The same can be defined for the two-dimensional system for the entropic case. We consider that the probability of getting a particle at position (q_x,q_y) and at time t be given by $P(q_x,q_y,t)$ for the system with an entropic barrier. Thus the response function can be defined as

$$P_i(t) = \int_{B_l(q_x)}^{B_u(q_x)} dq_y \int_{q_{x0}}^{\pm q_{xr}} dq_x\, P(q_x,q_y,t). \qquad (3.2)$$

The subscript i has the same implication as before; $i = L,R$ are used to designate the left and right lobes of the structure, respectively. Here one has to perform double integration as the space is two dimensional. In addition, q_{x0} represents the middle point of the bottleneck and $\pm q_{xr}$ are the extreme right and left ends of the structure, respectively. To obtain $P_L(t)$ one has to integrate between the limits q_{x0} and $-q_{xr}$ and to get $P_R(t)$ integration is from q_{x0} to q_{xr}. In this case also, $P_i(t)$ takes care of the total number of particles in left or right lobe. This integrated probability serves as the response function to explore hysteresis. For further analysis, we must concentrate on the normalized integrated probability of residence of the particles in one well or lobe. We numerically calculate the normalized integrated probability using Eq. (2.8) along with the equations of motion for the chaotic bath for the energetic case. To get the response function for the entropic case, we numerically solve Eq. (2.13) again with the bath dynamics along with the consideration of the confinement [Eq. (2.14)]. For the numerical integration, we have used an improved Euler algorithm, taking the time step $\Delta t = 10^{-3}$. To exploit the sensitive dependence on the initial conditions of the chaotic trajectories, we perform an average over 10^5 initial conditions of the bath variables. We use the following parameter sets: For the potential well we use the ratio $a_1{:}b_1 = 1{:}1$ and for the two-dimensional system $\epsilon{:}b = 25{:}2$.

The response function $P_L(t)$ is plotted against the oscillating part of the periodic force $\sin(\omega t)$ for both the energetic [Fig. 3(a)] and entropic [Fig. 4(a)] systems for several values of the frequency of oscillation ω. The integrated probability of residence of a particle in the left lobe $P_L(t)$ forms a closed loop when plotted against the oscillatory drive. The periodic force acting on the particles alternately increases and decreases with time. As expected, the response function also evolves with time in the same manner, i.e., in a periodic fashion. However, the interesting thing is that during the forward and backward movement of the response function, the same path is not followed. The frequency of oscillation is almost the same for the external drive and the response function, but the phase is different. The response function suffers a phase lag as if it retains a memory of its path. For example, consider that with the oscillatory force the response function decreases with time and at one point the periodic force begins to increase; thus it is expected that the response of the system towards the external drive would be instantaneous; however, this is not actually the case. The response function decreases for some more time before it realizes the increment of the oscillatory drive. This brings about the formation of the hysteresis loops. A symmetry breaking of the travel path of the response function occurs around its equilibrium value ($\frac{1}{2}$). The dynamical hysteresis occurs in the system as a result of competition between two time scales. One is the time period of oscillation of the external forcing and the other is the relaxation time of the system towards this drive in the presence of an energetic or entropic barrier. The relaxation time is determined by the bath to which the system is connected. In all previous cases dynamical hysteresis has been studied in the presence of thermal noise in the system. This random noise has a stochastic origin. In the present work, however, we focus on the point that the relaxation time of the system under study is affected by the chaotic dynamics of the bath, which has a deterministic origin. Thus the hysteresis loops observed can be termed deterministic hysteresis loops. Another interesting thing is that chaos-induced hysteresis loops can be observed for both energetic and entropic barriers.

The shape and size of the hysteresis loops for the left and right lobes are similar; only their orientations are different. This is evident from Figs. 3(b) and 4(b). The shape, size, and orientation of the hysteresis loops are very much dependent on the frequency of oscillation [Figs. 3(a) and 4(a)]. The dynamical hysteresis can occur when the time scales modulating the

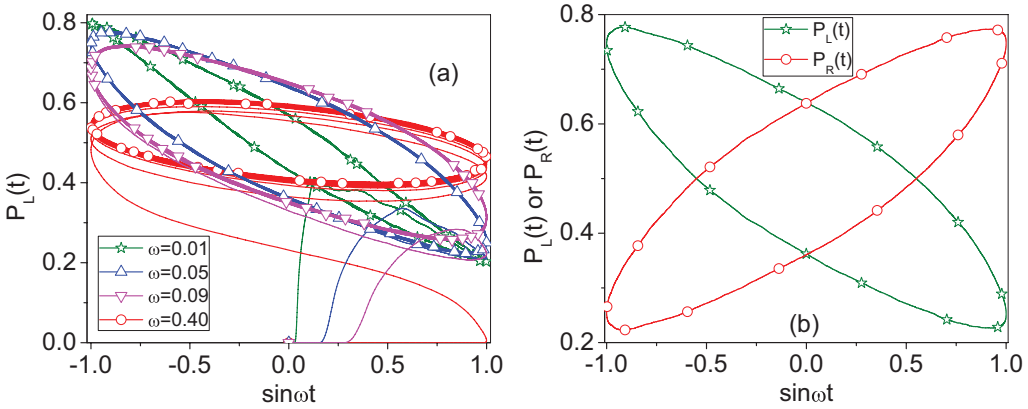

FIG. 3. (Color online) (a) Hysteresis loops in the presence of an energy barrier for different values of frequency ω for $A_0 = 0.4$. (b) Hysteresis loops for left and right lobes at a particular frequency $\omega = 0.05$ and amplitude $A_0 = 0.4$.

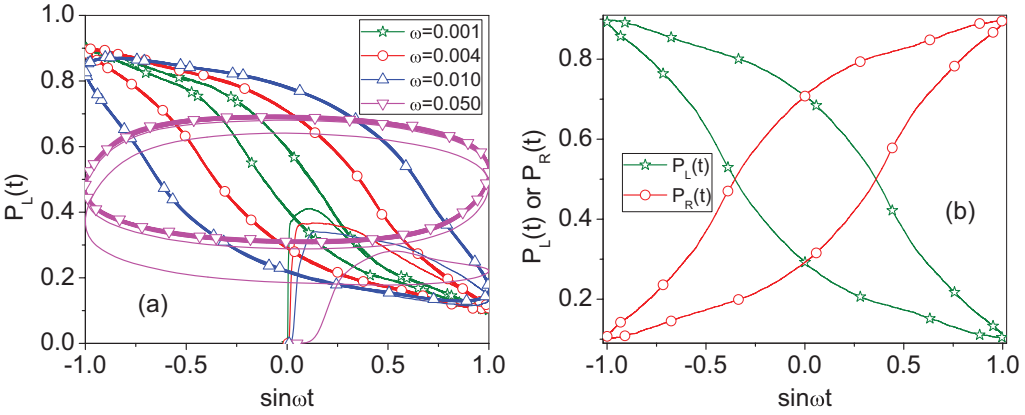

FIG. 4. (Color online) (a) Hysteresis loops in the presence of an entropic barrier for different values of frequency ω for $A_0 = 1.0$. (b) Hysteresis loops for left and right lobes at a particular frequency $\omega = 0.004$ and amplitude $A_0 = 1.0$.

systems are not very different and disappears in the static limit. The competition between the two time scales is most effective when they are comparable. When the frequency of modulation ω is very small, the time scales differ greatly; the response function traverses along almost the same path. The same is true when ω is very large. Then the response function evolves around a steady value $(\frac{1}{2})$ as the system relaxes much faster than the time period of oscillation of the drive. However, when the time scales are comparable, the system retains its memory for a much longer time. As a result, the paths for back and forth motion become very different. This gives rise to a large hysteresis loop.

Before proceeding to the following section, two pertinent points are noteworthy. We have considered a flat distribution of variables for random initial conditions in our numerical study. We have carried out numerical analysis with other distributions also. It has been found that the occurrence of hysteresis loops is independent of the distribution of variables, but the size of the loop is dependent on the width of distribution. In addition, we would like to mention that in order to check the validity of the present results the calculations have been done for the regular regime. The hysteresis is not observed in this case, implying that the chaotic motion of the bath dynamics plays a key role in bringing about hysteresis.

B. Hysteresis loop area

The deterministic hysteresis that we observe in the presence of energetic and entropic barriers can be quantified in terms of a dynamic order parameter such as the quantity $R_{hys}(\omega)$, which is defined as the integrated value of the response function $P_i(t)$ over a complete period, i.e., the area covered by the hysteresis loop. This is represented as

$$R_{hys}(\omega) = \oint P_i(t) dA, \tag{3.3}$$

where $A = A_0 \sin(\omega t)$. As discussed in the preceding section, the loop area would be maximum when the time scales governing the systems are comparable. This is what is reflected in the numerical calculation of the loop area. It has been

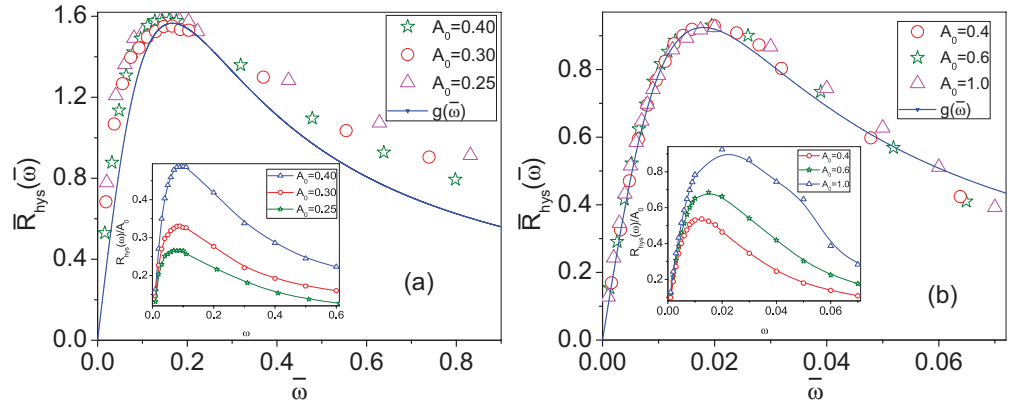

FIG. 5. (Color online) (a) Scaled loop area $\bar{R}_{hys} = R_{hys}/A_0^{\alpha}$ against scaled frequency $\bar{\omega} = \omega/A_0^{\gamma}$ in the presence of an energetic barrier. The inset shows the loop area R_{hys} scaled by the amplitude A_0 vs the driving frequency ω plot for three different values of the dimensionless amplitude A_0 in the presence of an energetic barrier; $g(\bar{\omega})$ is the fitting function and has the form $g(\bar{\omega}) = \frac{k_1\bar{\omega}}{1+k_2\bar{\omega}^2}$, with $k_1 = 18.8$ and $k_2 = 36.04$. (b) Scaled loop area $\bar{R}_{hys} = R_{hys}/A_0^{\alpha}$ against scaled frequency $\bar{\omega} = \omega/A_0^{\gamma}$ in the presence of an entropic barrier. The inset shows the loop area R_{hys} scaled by the amplitude A_0 vs the driving frequency ω plot for three different values of the scaled amplitude A_0 in the presence of an entropic barrier; $g(\bar{\omega})$ is the fitting function and has the form $g(\bar{\omega}) = \frac{k_1\bar{\omega}}{1+k_2\bar{\omega}^2}$, with $k_1 = 103.0$ and $k_2 = 3100.0$.

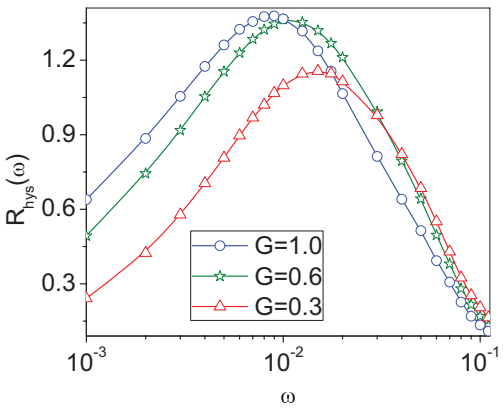

FIG. 6. (Color online) Loop area R_{hys} vs the driving frequency ω plot for three different values of G.

found that the loop area tends to zero for very low and very high frequencies and is maximum at an intermediate value. The quantity R_{hys} shows a turnover when plotted against the frequency of oscillation ω. We have plotted the hysteresis loop area R_{hys} against ω for three different values of amplitude of oscillation for both the energetic [inset of Fig. 5(a)] and entropic [inset of Fig. 5(b)] systems. In both cases it is shown that the loop area increases with an increase in amplitude of oscillation. Another observation is that the position of the turnover shifts towards the right with increasing amplitude. This implies that the relaxation time scale of the system is also influenced by the amplitude through the nonlinearity of the system and bath dynamics.

For the entropic system G is a parameter that can be used to tune the system between entropy- and energy-dominated regimes. We have plotted R_{hys} against ω for different values of G (Fig. 6). It has been found that the maximum of R_{hys} vs ω curve shifts towards the left with increasing values of G.

C. Scaling relations

It has been discussed earlier that the hysteresis loop area vanishes in the very-low- and very-high-frequency limits. The observed variation can be fitted in the form

$$R_{hys}(\omega) = A_0^{\alpha}\omega^{\beta} g\left(\frac{\omega}{A_0^{\gamma}}\right), \tag{3.4}$$

with the scaling exponents α, β, and γ. Here g is the scaling function that vanishes when the argument of the function tends to 0 or ∞. It is well known [1] that the exponents depend predominantly on the dynamic process involved and also on the ranges of frequency and amplitude. Since under a linear approximation the loop area vs ω plot fits a Lorentzian curve [1], we consider the scaling function g of a Lorentzian form in the low-frequency limit. We scale the frequency by A_0^{γ} and g is the function of the scaled frequency. The loop area variation is represented by the expression

$$R_{hys}(\bar{\omega}) = A_0^{\alpha}\frac{k_1\bar{\omega}}{1+k_2\bar{\omega}^2}, \tag{3.5}$$

where $\bar{\omega} = \frac{\omega}{A_0^{\gamma}}$ and $g(\bar{\omega}) = \frac{k_1\bar{\omega}}{1+k_2\bar{\omega}^2}$. So the scaled area is

$$\bar{R}_{hys}(\bar{\omega}) = R_{hys}(\bar{\omega})/A_0^{\alpha}. \tag{3.6}$$

If we plot the scaled loop area against the scaled frequency for different amplitudes, all the curves collapse on a single Lorentzian for both energetic [Fig. 5(a)] and entropic [Fig. 5(b)] barriers. For the system with an energy barrier, the values of the exponents are $\alpha = 2.285$ and $\gamma = 0.51$. For the system with an entropic barrier, $\alpha = 1.6$ and $\gamma = 0.51$. The hysteresis loop area therefore satisfies a scaling law with exponents that depend on the nature of the barrier.

Finally, a discussion about the nature of dynamical hysteresis in relation to a cooperatively interacting system (e.g., a ferromagnetic system represented by the Ising model with nearest-neighbor ferromagnetic coupling) is pertinent. We begin by noting that the ferromagnetic system is a many-body system, whereas we are dealing here with a few-body system. The origin of relaxational delay in a few-body system and in a many-body system is different. The response magnetization in the latter case captures the basics of dynamical hysteresis within a mean field description. The response function in our study is the integrated probability of residence of the particles in one of the wells or lobes in the sense of an average (over the ensemble) in the spirit of mean field. The observed scaling behavior (which manifestly characterizes the dynamical transition in a many-body system) in the present study is another hint towards the similarity of the two scenarios, but does not stem from interacting cooperation *per se*. Another aspect of dynamical hysteresis is that the variation of loop area as a function of frequency is reminiscent of the stochastic resonance phenomenon where the turnover in the rate of escape (inverse of the mean first-passage time) is observed due to the periodic oscillation of the effective energetic and entropic barriers. However, a careful analysis reveals [53] that the loop area essentially takes care of the average effect that includes not only the mean first-passage time but also the higher moments. Thus the observed effect is distinct from stochastic resonance.

IV. CONCLUSION

Although static hysteresis as a result of the equilibrium response of a cooperatively interacting many-body system, such as a magnet, has been well known for a long time, the nonequilibrium response of the system to a time-dependent drive has been the subject of more recent research. We have explored this nonequilibrium response when the periodically driven system in question is kept in contact with a chaotic bath, i.e., a few degree-of-freedom dynamical system. Two distinct situations governed by energetic and entropic barriers have been considered. Dynamical hysteresis carries the signature of the nonequilibrium response in terms of closed loops of a nonvanishing area in the response-function–periodic-drive plot; the response function characterizes the probability of finding the particle in one of the two wells of the double-well potential (for the energetic case) or in one of the two lobes of a bilobal enclosure (for the entropic case). It has been shown that the hysteresis effect is optimal when the hysteresis loop area exhibits a maximum at a given frequency of the drive and vanishes in the static limit. The analysis of the variation of the hysteresis loop area with frequency reveals a generic form that can be captured by appropriate scaling relations. The scaling exponents for the energetic and the entropic barriers

are different, implying the distinctive nature of the underlying dynamical processes in the two cases. Our analysis shows that the memory effect under the influence of the deterministic noise of a dynamical system can play a decisive role in the dynamic response even for a few-degrees-of-freedom system.

ACKNOWLEDGMENTS

M.D. would like to thank Dr. Debasish Mondal for helpful discussions. Thanks are due to the Council of Scientific & Industrial Research, Government of India, for partial financial support.

[1] B. K. Chakrabarty and M. Acharyya, Rev. Mod. Phys. **71**, 847 (1999).
[2] C. N. Luse and A. Zangwill, Phys. Rev. E **50**, 224 (1994); Y. L. He and G. C. Wang, Phys. Rev. Lett. **70**, 2336 (1993); A. M. Somoza and R. C. Desai, *ibid*. **70**, 3279 (1993).
[3] M. C. Mahato and S. R. Shenoy, Phys. Rev. E **50**, 2503 (1994).
[4] Lin I and J.-M. Liu, Phys. Rev. A **46**, R733 (1992).
[5] A. Hohl, H. J. C. van der Linden, R. Roy, G. Goldsztein, F. Broner, and S. H. Strogatz, Phys. Rev. Lett. **74**, 2220 (1995); P. Jung, G. Gray, R. Roy, and P. Mandel, *ibid*. **65**, 1873 (1990).
[6] G. Trefan, P. Grigolini, and B. J. West, Phys. Rev. A **45**, 1249 (1992).
[7] V. L. Berdichevsky and M. V. Alberti, Phys. Rev. A **44**, 858 (1991).
[8] B. C. Bag, J. Ray Chaudhuri, and D. S. Ray, J. Phys. A: Math. Gen. **33**, 8331 (2000).
[9] S. Chaudhuri, G. Gangopadhyay, and D. S. Ray, Phys. Rev. E **47**, 311 (1993); **52**, 2262 (1995).
[10] S. Mukamel, V. Khidekel, and V. Chernyak, Phys. Rev. E **53**, R1 (1996); B. C. Bag and D. S. Ray, *ibid*. **62**, 1927 (2000).
[11] R. Zwanzig, J. Phys. Chem. **96**, 3926 (1992).
[12] M. H. Jacobs, *Diffusion Processes* (Springer, New York, 1967).
[13] H. Zhou and R. Zwanzig, J. Chem. Phys. **94**, 6147 (1991); R. Zwanzig, Physica A **117**, 277 (1983).
[14] D. Reguera and J. M. Rubi, Phys. Rev. E **64**, 061106 (2001).
[15] D. Reguera, G. Schmid, P. S. Burada, J. M. Rubi, P. Reimann, and P. Hänggi, Phys. Rev. Lett. **96**, 130603 (2006); P. S. Burada, G. Schmid, D. Reguera, J. M. Rubi, and P. Hänggi, Phys. Rev. E **75**, 051111 (2007).
[16] D. Mondal and D. S. Ray, Phys. Rev. E **82**, 032103 (2010).
[17] P. S. Burada, G. Schmid, P. Talkner, P. Hänggi, D. Reguera, and J. M. Rubi, BioSystems **93**, 16 (2008).
[18] D. Mondal, M. Das, and D. S. Ray, J. Chem. Phys. **133**, 204102 (2010).
[19] P. S. Burada, G. Schmid, D. Reguera, M. H. Vainstein, J. M. Rubi, and P. Hänggi, Phys. Rev. Lett. **101**, 130602 (2008); P. S. Burada, G. Schmid, D. Reguera, J. M. Rubi, and P. Hänggi, Eur. Phys. J. B **69**, 11 (2009).
[20] D. Mondal, M. Das, and D. S. Ray, J. Chem. Phys. **132**, 224102 (2010).
[21] B. Q. Ai and L. G. Liu, J. Chem. Phys. **126**, 204706 (2007); Phys. Rev. E **74**, 051114 (2006).
[22] D. Mondal, Phys. Rev. E **84**, 011149 (2011).
[23] F. Marchesoni and S. Savelev, Phys. Rev. E **80**, 011120 (2009); M. Borromeo and F. Marchesoni, Chem. Phys. **375**, 536 (2010).
[24] M. Das, D. Mondal, and D. S. Ray, J. Chem. Sci. **124**, 21 (2012).
[25] D. Mondal and D. S. Ray, J. Chem. Phys. **135**, 194111 (2011); D. Mondal, M. Sajjan, and D. S. Ray, J. Indian Chem. Soc. **88**, 1791 (2011).
[26] B. Q. Ai and L. G. Liu, J. Chem. Phys. **128**, 024706 (2008); B. Q. Ai, H. Z. Xie, and L. G. Liu, Phys. Rev. E **75**, 061126 (2007).
[27] B. Q. Ai, J. Chem. Phys. **131**, 054111 (2009).
[28] M. Borromeo, F. Marchesoni, and P. K. Ghosh, J. Chem. Phys. **134**, 051101 (2011).
[29] F. Marchesoni, J. Chem. Phys. **132**, 166101 (2010).
[30] M. Das, D. Mondal, and D. S. Ray, Phys. Rev. E **86**, 041112 (2012).
[31] A. M. Berezhkovskii, M. A. Pustovoit, and S. M. Bezrukov, Phys. Rev. E **80**, 020904(R) (2009); A. M. Berezhkovskii and S. M. Bezrukov, Biophys. J. **88**, L17 (2005).
[32] M. Muthukumar, J. Chem. Phys. **118**, 5174 (2003); Phys. Rev. Lett. **86**, 3188 (2001); J. K. Wolterink, G. T. Barkema, and D. Panja, *ibid*. **96**, 208301 (2006).
[33] W. Sung and P. J. Park, Phys. Rev. Lett. **77**, 783 (1996); P. J. Park, and W. Sung, *ibid*. **80**, 5687 (1998); K. Luo, T. Ala-Nissila, S.-C. Ying, and A. Bhattacharya, *ibid*. **99**, 148102 (2007); **100**, 058101 (2008).
[34] J. A. Cohen, A. Chaudhuri, and R. Golestanian, Phys. Rev. Lett. **107**, 238102 (2011).
[35] S. Van Dorp, U. F. Keyser, N. H. Dekker, C. Dekker, and S. G. Lemay, Nat. Phys. **5**, 347 (2009); Z. Siwy and A. Fulinski, Phys. Rev. Lett. **89**, 198103 (2002); Z. Siwy, I. D. Kosinska, A. Fulinski, and C. R. Martin, *ibid*. **94**, 048102 (2005).
[36] P. Kalinay and J. K. Percus, Phys. Rev. E **72**, 061203 (2005); **74**, 041203 (2006); J. Stat. Phys. **123**, 1059 (2006).
[37] P. Kalinay and J. K. Percus, J. Chem. Phys. **122**, 204701 (2005).
[38] A. M. Berezhkovskii, M. A. Pustovoit, and S. M. Bezrukov, J. Chem. Phys. **126**, 134706 (2007).
[39] A. M. Berezhkovskii, V. Yu. Zitserman, and S. Y. Shvartsman, J. Chem. Phys. **118**, 7146 (2003); **119**, 6991 (2003); O. K. Dudko, A. M. Berezhkovskii, and G. H. Weiss, J. Phys. Chem. B **109**, 21296 (2005).
[40] L. Dagdug, Alexander M. Berezhkovskii, Y. A. Makhnovskii, V. Y. Zitserman, and S. M. Bezrukov, J. Chem. Phys. **134**, 101102 (2011).
[41] A. M. Berezhkovskii and L. Dagdug, J. Chem. Phys. **134**, 124109 (2011).
[42] A. M. Berezhkovskii, L. Dagdug, Y. A. Makhnovskii, and V. Y. Zitserman, J. Chem. Phys. **132**, 221104 (2010).
[43] L. Dagdug, M. V. Vazquez, A. M. Berezhkovskii, and S. M. Bezrukov, J. Chem. Phys. **133**, 034707 (2010).
[44] A. M. Berezhkovskii and L. Dagdug, J. Chem. Phys. **133**, 134102 (2010).
[45] K. K. Mon, J. Chem. Phys. **130**, 184701 (2009).
[46] Y. A. Makhnovskii, A. M. Berezhkovskii, and V. Y. Zitserman, J. Chem. Phys. **131**, 104705 (2009).

[47] M. V. Vazquez, A. M. Berezhkovskii, and L. Dagdug, J. Chem. Phys. **129**, 046101 (2008).
[48] K. K. Mon, J. Chem. Phys. **128**, 124711 (2008).
[49] A. M. Berezhkovskii, A. V. Barzykin, and V. Y. Zitserman, J. Chem. Phys. **131**, 224110 (2009).
[50] K. K. Mon and J. K. Percus, J. Chem. Phys. **125**, 244704 (2006); K. K. Mon, *ibid*. **128**, 197102 (2008); P. Kalinay, *ibid*. **126**, 194708 (2007); **128**, 197103 (2008).
[51] S. B. Chen, J. Chem. Phys. **134**, 014902 (2011); **135**, 014904 (2011).
[52] D. Mondal, M. Das, and D. S. Ray, Phys. Rev. E **85**, 031128 (2012).
[53] M. Das, D. Mondal, and D. S. Ray, J. Chem. Phys. **136**, 114104 (2012).
[54] Z. Schuss, A. Singer, and D. Holcman, Proc. Natl. Acad. Sci. USA **104**, 16098 (2007).
[55] O. Benichou, C. Chevalier, J. Klafter, B. Meyer, and R. Voituriez, Nat. Chem. **2**, 472 (2010).
[56] O. Benichou and R. Voituriez, Phys. Rev. Lett. **100**, 168105 (2008).
[57] P. K. Ghosh, F. Marchesoni, S. E. Savelev, and F. Nori, Phys. Rev. Lett. **104**, 020601 (2010).
[58] P. K. Ghosh, R. Glavey, F. Marchesoni, S. E. Savelev, and F. Nori, Phys. Rev. E **84**, 011109 (2011).
[59] M. A. Marchiori, R. Fariello, and M. A. M. de Aguiar, Phys. Rev. E **85**, 041119 (2012).
[60] H. Risken, *The Fokker-Planck Equation*, 2nd ed. (Springer, Berlin, 1989).